Original Article

Flexibility Analysis of *Bacillus thuringiensis* Cry1Aa*

ZHAO Xin Min[1,2,#], XIA Li Qiu[2], YANG Xiao Ping[1,3], and PENG Xiao Yun[1]

1. Department of Chemistry and Environmental Engineering, Hunan City University, Yiyang 413000, Hunan, China; 2. Key Laboratory of Microbial Molecular Biology of Hunan Province, College of Life Science, Hunan Normal University, Changsha 410081, Hunan, China; 3. Division of Medical Oncology, Department of Medicine, School of Medicine, University of Colorado Anschutz Medical Campus, Aurora, USA

Abstract

Objective To investigate the flexibility and mobility of the *Bacillus thuringiensis* toxin Cry1Aa.

Methods The graph theory-based program Constraint Network Analysis and normal mode-based program NMsim were used to analyze the global and local flexibility indices as well as the fluctuation of individual residues in detail.

Results The decrease in Cry1Aa network rigidity with the increase of temperature was evident. Two phase transition points in which the Cry1Aa structure lost rigidity during the thermal simulation were identified. Two rigid clusters were found in domains I and II. Weak spots were found in C-terminal domain III. Several flexible regions were found in all three domains; the largest residue fluctuation was present in the apical loop2 of domain II.

Conclusion Although several flexible regions could be found in all the three domains, the most flexible regions were in the apical loops of domain II.

Key words: Flexibility; Cry1Aa; *Bacillus thuringiensis*; Constraint Network Analysis; NMSim

Biomed Environ Sci, 2015; 28(9): 634-641 *doi: 10.3967/bes2015.089* *ISSN: 0895-3988*

www.besjournal.com (full text) *CN: 11-2816/Q*

INTRODUCTION

Proteins rely on flexibility to execute their biological functions by interacting with either large biomolecules or small biomolecules[1]. These interactions need a certain degree of conformational adaptation in order to better complement the binding partners[2]. For example, insulin shows conformational flexibility in two major forms, R-state and T-state[3-4]. The R-state, an inactive form with residues B1-B8, is in an α-helical conformation while the active, T-state with residues B1-B8, is in an extended conformation, which exposes the hydrophobic core region of insulin chain-B, long suspected to be involved in receptor binding. Additionally, flexibility (and its opposite, rigidity) plays an important role for a protein's structural stability[5] and information on protein flexibility is increasingly used in computer-aided drug discovery and molecular design[6].

Although experimental techniques for studying protein structures, particularly protein flexibility, have received great progress, theoretical methods have been recognized as efficient yet as difficult tools to solve this puzzle. One of the most powerful theoretical methods is the atomic molecular dynamics

*This study was supported by grants from the National Natural Science Foundation of China (No. 30670052) and 863 Program of China (No. 2006AA02Z187).

#Correspondence should be addressed to ZHAO Xin Min, professor, Tel: 86-737-6353033, Fax: 86-737-6353045, E-mail: zhaoxmcn@163.com

Biographical note of the first author: ZHAO Xin Min, male, born in 1962, PhD, major in molecular microbiology.

(MD)[7], a strong method that provides accurate representations of protein flexibility under physiological-mimic environments. MD is a complex, computationally expensive method, where its utilization needs a certain degree of expertise[8]. Normal mode analysis can quickly reveal the overall change in the conformation of large proteins; it is unnecessary to calculate the specific molecular mechanism such as the motion of specific bonds. In particular, normal modes analysis is able to perform low-frequency modes that describe the large-scale, overall motion of the protein. Many normal mode analysis servers are available such as NOMAD-ref[9], Elnemo[10], Flexserv[11], Webnm[12], ANM[13], and iMODS[14]. However, some of those methods are based on Cartesian space and are limited to use. The other methods do not generate actual structures or do not respect the most basic geometric constraints of bond angles and distances. ENCoM was recently developed to predict the effect of mutations on the thermodynamic stability of a structure using vibrational entropy calculations[15].

Here we used two programs, Constraint Network Analysis (CNA)[16] and NMSim[17], to verify Cry1Aa flexibility and mobility. CNA is a graph theory-based rigidity analysis that evaluates global and local flexibility and rigidity characteristics of proteins. NMSim is a graph theoretical approach based on normal mode analysis to simulate actual protein movements. These two programs are available in web servers and are easy to use.

Bacillus thuringiensis (Bt) strains produce a rather diverse group of toxin proteins[18]. Most of those delta-endotoxins belong to the Cry (crystal) family of proteins. They are highly specific to their target insects and innocuous to humans, vertebrates and plants. They are completely biodegradable and widely used in agriculture as a biopesticide. Cry1Aa was isolated from Bt subsp. *Kurstaki*[19] and is active against easy-bleeding insect *Bombyx mori* and the forest pest *Lymantria dispar.*

Due to the importance of these Cry toxins, several crystal structures, including Cry1Aa, have been elucidated and reviewed recently[20]. It is well known that all Cry toxins contain three structural domains and share a high degree of topological similarity. The overall 3D structures of these toxins are very similar; all consisting of three structurally conserved domains. The domain I consists of seven alpha helices in which helix 5 is surrounded by the others, forming a helical bundle. Several studies have confirmed that this domain is responsible for channel ion formation[21-22]. The domain II is formed by three antiparallel β-sheets joined in a Greek key topology arranged in a β-prism. Its function is associated with receptor recognition and binding[23]. The domain III is formed by two anti-parallel β-sheets constituting a β-sandwich in a jelly roll topology. The function of this domain is unclear but it seems to be important to the toxin stability, and it has been found to participate in the determination of toxin specificity[24-25]. Although Cry toxins have been widely used commercially, the details of their mode of action remain controversial.

We selected Cry1Aa, whose 3D structure has been determined, as the target for our investigation because it is one of the most characterized Cry toxins regarding its biological function and action mechanism[19]. It is also a commercialized transgenic insecticide with excellent activity[18]. Furthermore, detailed information about the flexibility of Cry1Aa will provide hints about where the introducing mutations may improve the stability and lead to a deep understanding of the action mechanism of Cry toxins.

MATERIALS AND METHODS

Cry1Aa structure was retrieved from Protein Data Bank database (PDB code: 1CIY). Flexibility analysis of Cry1Aa was performed using CNA which is a graph theory-based rigidity analysis that detects global and local flexibility and rigidity features of proteins by carrying out thermal unfolding simulations[26-27]. CNA performs the thermal unfolding simulations based on the graph theory. In the network, the number of hydrophobic contacts is stably maintained or increased to treat hydrophobic interactions in a temperature-dependent mode. During the simulation, the noncovalent constraints are removed from the initial network. This means that for a given network state s=f(*T*), hydrogen bonds (including salt bridges) with an energy $E_{hb}>E_{cut,hb}$ are removed from the network. Thereafter, rigid cluster decomposition is operated on each constraint network state (s).

Phase transition points were identified on the basis of the global indices during the thermal unfolding simulation. The global index changes rapidly corresponding to the $E_{cut,hb}$ that indicates a network shift from being largely rigid to largely flexible. Such a shift can be related to the folded-unfolded transition for a protein. The changes of flexibility related to the indices as a function of temperature can be obtained; for this, $E_{cut,hb}$ was converted to a temperature scale

using a linear relation: T=-20K/(kcal/mol) $E_{cut,hb}$+300K[28]. The main characteristic of CNA is that it allows performing and analyzing thermal in spectacular detail, which provides the highest advantage from information on biomolecular flexibility by linking results to biologically relevant features of a structure, such as thermalstability and function[16]. CNA has been shown to be succesful in investigating protein thermalstability and structure weak spot[16]. CNA correctly predicts which one of the two proteins is more thermalstable for two thirds of a data of 19 pairs of proteins from mesophilic and thermophilic organisms[29]. However, CNA only reflects what can move in a protein but does not simulate actual protein movements. To characterize protein movement, NMSim program was used. The NMSim web server combines graph theory with normal mode analysis. Firstly, the input structure is simulated using the FIRST software based on graph theory[30-31]. Secondly, low-frequency normal modes are yielded by normal made analysis. Finally, a stereochemically valid conformation from the distorted structure was generated by moving the structure along with the directions of low-frequency normal modes. The key feature of NMSim is that the generated structures are iteratively corrected regarding steric clashes and stereochemical constraint violations.

To compute global and local flexibility indices of Cry1Aa, default parameters were used for the CNA analysis. For NMSim analysis, small-scale motion was selected for the simulation type with the other parameters defaulted.

RESULTS

Global Flexibility Indices

Global flexibility indices characterize the degree of flexibility and rigidity within the constraint system at a macroscopic level[32]. During the thermal unfolding simulation, these global indices are calculated for each network state (s). Global indices allow the identification of phase transition points (points in which these indices change sharply during the thermal unfolding simulation) that relate to the folded-unfolded transitions of proteins. Four global flexibility indices, including floppy mode density, mean rigid cluster size, rigidity order parameter, and phase transition points were calculated.

The Floppy Mode Density Φ refers to the number of internal independent degrees of freedom that are associated with dihedral rotations, normalized by the number of overall internal degrees of freedom associated with the total number of bodies in the network[32]. In the current case (Figure 1A), the increase of floppy mode density of Cry1Aa with increasing temperature (equivalent to a decreasing $E_{cut,hb}$) is evident, indicating that Cry1Aa is gradually getting more 'floppy'.

Mean Rigid Cluster Size S originated from percolation theory, moments of the size distribution of rigid clusters can be used to analyze macroscopic properties of constraint networks[32]. Here S represents the mean rigid cluster size; the size of the largest rigid cluster is always excluded from the calculation, which results in S being zero as long as one rigid cluster dominates the whole network or if all rigid clusters disappear. In this analysis, the mean rigid cluster size S shows to be near zero at high $E_{cut,hb}$ because even the largest cluster cover the whole network. By removing hydrogen bond constraints from the network, the rigid cluster starts to decay, which leads to a steep increase of S at -1.27 kcal/mol (Figure 1B). Thereafter, S starts to decrease because the system becomes less and less dominated by rigid components.

The Rigidity Order Parameter P_∞ indicates the fraction of the network belonging to the giant percolating cluster[32]. During the simulation, the melting of the giant percolating cluster is detected and the largest rigid subcluster of the previous giant percolating cluster falls into the new giant percolating cluster of the present network state (s). As long as the network is in the rigid phase, it is dominated by one rigid cluster and therefore, P_∞ is close to one. In the floppy phase, with a vanishing largest rigid cluster, P_∞ decreases to zero.

In Figure 1C, a sharp decline at $E_{cut,hb}$=−1.27 kcal/mol can be identified. $E_{cut,hb}$=−1.27 kcal/mol amounts to 325.32 K.

Cluster Configuration Entropy H was introduced by Andraud et al. as a morphological descriptor for heterogeneous materials[33]. The cluster configuration entropy H is a measure of the disorder degree in the realization of a given network state[32]. In Figure 1D, two phase transition points during the thermal unfolding simulation are monitored. The early phase transition point at $E_{cut,hb}$=−1.27 kcal/mol in H profile is equivalent to the temperature of 325.32 K. However, a late transition at $E_{cut,hb}$=−2.27 kcal/mol (or, equivalently 345.43 K) in H profile can also be identified, which represents the final substantial decay of the rigid core.

The decay of the giant rigid cluster occurs by multiple steps in a hierarchical fashion (Figure 1C and

1D).

Local Index- Percolation Index (p_i)

Local flexibility index monitors the degree of flexibility and rigidity within the constraint system at a microscopic level[32]. Usually, the local index for a residue indicates the network state (s) during the simulation when the residue becomes flexible from prior rigidity. Percolation index, p_i, is a local parameter similar to the rigidity order parameter P_∞; it monitors the percolation behavior of a biomolecule at a microscopic level. As such, it can identify the hierarchical organization of the giant percolating cluster during the thermal unfolding simulation. The value of p_i=0 indicates that an atom has never been part of the giant percolating cluster. The lowest p_i value then emphasizes the most stable subcomponent in the network.

In this case (Figure 2), two apparent flexible regions in domain I (residues 1-222) are detected; the first is a helix α2a (residues 33-38) and the second includes residues 125-128 that link helix α4 and α5. Three rigid regions (residues 172-178, 194-212, and 244-248) with lower percolation index piare then detected in the helix α3, α6, and α7 of domain I, respectively.

In domain II (residues 223-425), four flexible regions (residues 308-311, 336-342, 360-367 and 407-413) can be found. Three out of four flexible regions belong to apical loops of the domain. Another flexible region (residues 360-367) is included in a loop located in the back of the domain (Figure 2).

In domain III, three flexible regions (residues 457-460, 522-528, 545-547) can also be found.

Unfolding Nuclei

Unfolding nuclei can be regarded as weak spots[32]. Most Cry1Aa weak spots identified by CNA are located in the C-terminal β-sheet domain (Figure 3). Fifty residues are distributed in the region of residues 440-570 of domain III. These residues belong to the giant rigid cluster up till the phase transition point and, at this point, segregate from the giant rigid cluster. Hence, unfolding of the giant rigid cluster begins from these residues.

Stability Maps

Figure 4 shows that the structural stable elements in the C-terminal domain are somehow cross-linked. There is a weak stable box in the N-terminal domain, and some little blue boxes, which represent that strong rigidity regions are distributed in the domain I.

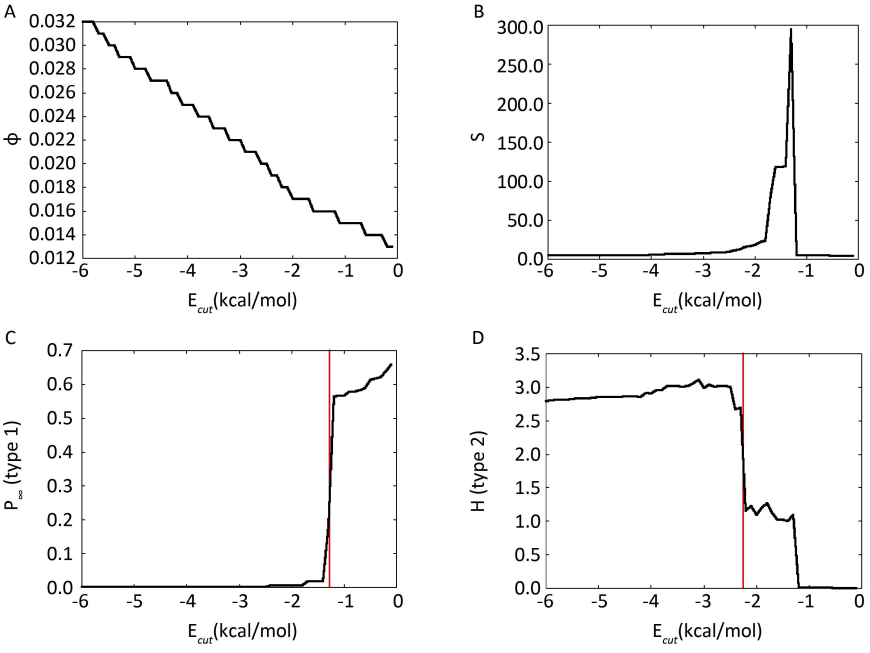

Figure 1. Global indices for the thermal unfolding of Cry1Aa as a function of the hydrogen bonding energy cutoff $E_{cut,hb}$: (A) floppy mode density Φ; (B) mean rigid cluster size S; (C) rigidity order parameter P_∞ type 1; (D) cluster configuration entropy H type 2. The red vertical lines (C-D) correspond to the identified phase transitions.

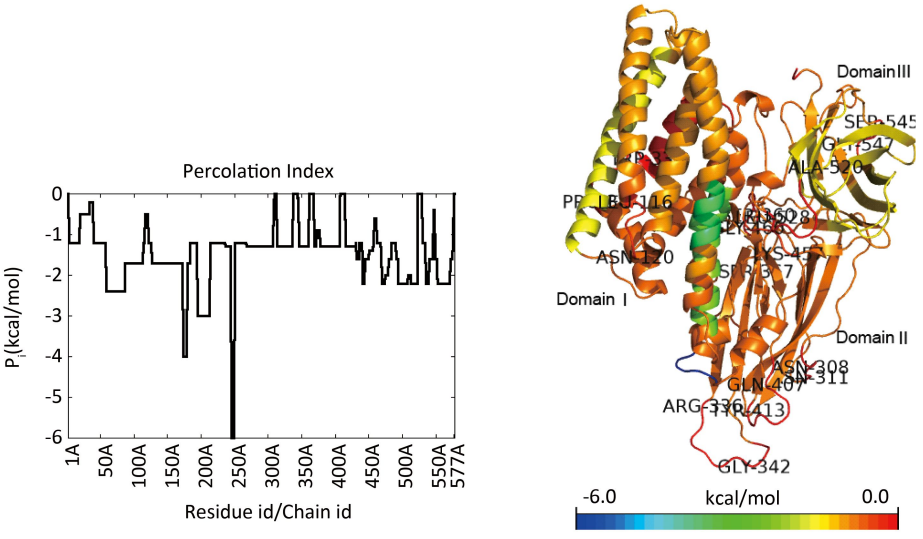

Figure 2. Percolation index p_i for Cry1Aa. The lower p_i value is the longer part of a residue of the giant percolating cluster during the thermal unfolding simulation. On the right, the respective indices are mapped onto the input structure in a color-coded manner.

Movements Simulation of Individual Residues

To study the fluctuation of individual residues in detail, the root-mean-square fluctuation (RMSF) of C-alpha atoms of Cry1Aa was analyzed by NMSim. Here the RMSF profile resembles that of the percolation index shown in Figure 5. Four comparative large movements are found in the apical loops of domain II. The largest fluctuation is found in loop 2.

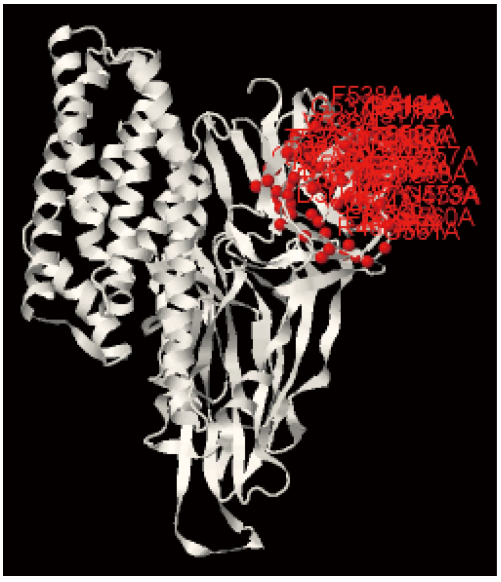

Figure 3. Red spheres represent weak spots in the Cry1Aa structure.

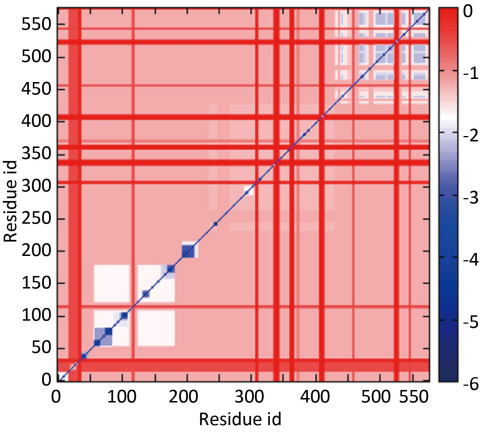

Figure 4. Stability map for Cry1Aa. Red colors indicate pairs of residues where no, or only a weak rigid contact exists. In contrast, blue colors indicate strong rigid contacts.

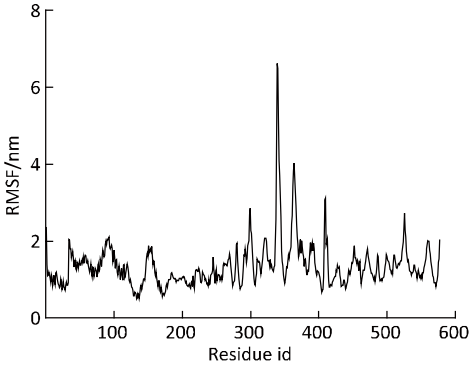

Figure 5. C-alpha RMSF per residues calculated for Cry1Aa.

DISCUSSION

Four global Cry1Aa indices reflect the flexibility in a general way; particularly two phase transition points during the thermal unfolding simulation can be monitored. At the first transition point, the Cry1Aa structure sharply loses rigidity on thermal unfolding, meaning that one terminal domain begins segregating from the giant cluster, although it is unconfirmed whether it is the N-terminal α-helix or the C-terminal β-sheet domain of Cry1Aa. Usually, the second transition point is related to a protein melting[32]. The reason for P_∞ and H behavior in a hierarchical fashion is that Cry1Aa is composed of multiple sub-domains that segregate from the giant cluster independently from each other.

Local flexibility index and the root-mean-square fluctuation (RMSF) of Cry1Aa C-alpha atoms describe the fluctuation of individual residues in detail.

At present, the most accepted model of Cry toxin is an 'umbrella' mode. In that action mode, the domain I forms a bundle of eight anti-parallel helices with helix α5 in the center; it is a helical bundle involved in membrane insertion, oligomerization, and pore formation. The hydrophobic hairpin formed by helices α4 and α5 inserts into the phospholipid bilayer whereas the rest of amphipathic helices of domain I are spread on the membrane surface in an umbrella-like conformation[34].

Helix α2a links helix α1 and α2b, and the flexibility of helix α2a likely makes it possible to free helix α1 from the rest of the domain. The flexible region linking helices α4 and α5 allows helices α1 to α4 to be conformed in a way that they are banged to the bundle. This conformation may be necessary at the onset of the membrane insertion process. The rigid regions in the helix α3, α6, and α7 indicate that those helices are rigid as an independent helix. It is reasonable to infer that it is necessary for the ion channel formation in the cell membrane, since the rigidity may be useful for insertion. Unsurprisingly, a transition region that shows the lowest p_i value between domain I and domain II is always part of a rigid cluster throughout the thermal unfolding simulation (Figure 2). This rigid region likely plays an important role in keeping the toxin in a compact globular form during solubilization and activation of the protoxin in the insect gut.

It is likely that the apical loops of the domain II participate in the receptor binding and hence in determining the specificity of the toxin for insect larvae. Site-directed mutagenesis of the loop residues in the related toxins was reported to affect binding affinity and toxicity[23,35]. Simulation here suggests that these residues are flexible at the working temperature. Their flexibility is useful for binding, because this kind of conformational adaptation can do a better job matching the binding partner. An earlier study showed that the apical loop 2 of domain II is highly variable in length and amino acid sequence among Cry1Aa, Cry2Aa, Cry3Aa, Cry4Aa, and Cry5Aa toxins[36]. The reason they share different insect specificity is that those toxins target different midgut surface receptors, or target different kinds of specificity determinants on shared receptors with structurally similar apical loops[25]. We therefore infer that the flexibility of the apical loops, particularly loop 2, is important in the toxin-receptor complex formation. A recently study showed that loop 1, loop 2, and loop 3 of Cry1Aa toxin's domain II were involved in toxin-BtR175 receptor binding[37]. In another reported study, the flexibility of a loop in *Escherichia coli* class H fructose-1.6-bisphophate aldolase was found to be important to its catalytic activity[38], and similar phenomenon was also found in the nucleotide hydrolase from *Trypanosoma vivax*[39].

In Figure 2, it can be observed that the N-terminal domain is less stable than the C-terminal domain. Consequently, it is clear that the early phase transition points in P_∞ and H profiles explain that the Cry1Aa structure sharply lost rigidity on thermal unfolding when the N-terminal domain begins to segregate from the giant cluster. The giant percolating cluster, which at this point consists mainly of the β-sheet regions in the C-terminal domain III (residues 426-577), disintegrates into smaller clusters at the later phase transition point ($E_{cut,hb}$=−2.27 kcal/mol).

Weak spots of Cry1Aa are in the C-terminal domain, and they belong to the giant rigid cluster until the phase transition points segregate from it during the thermal unfolding simulation. Regarding the protein stability, giant rigid cluster unfolding begins from these residues. It is more possible that mutation of these residues makes this protein more stable. Domain III is a β-sandwich and it is implicated in both correct folding of the whole active toxin and receptor recognition[21]; it is also involved in stability[25]. Our previous studies showed that the mutant W544F of Cry1Ac Domain III, a close relative to Cry1Aa, was more stable than the wild type when preserved at room temperature[36-37]. Cry1Ac has similar structure and high sequence identity with Cry1Aa. It is reasonable that these residues in C-terminal domain of Cry1Aa can be used to increase the stability or even the toxicity of the toxin for molecular design.

In Cry1Aa domain III, a comparative large

flexibility region with the peak residue 525 can be found. This region is included in the loop that links β19-β20 of domain III. In an earlier study on Cry5a of *Bacillus thuringiensis*, results also showed that the apical loop2 was very flexible. The results of site-directed mutagenesis and truncation analysis provided strong evidence for the involvement of domain III in receptor binding and insecticidal activity[24-25,40-41]. This flexible region in domain III of Cry1Aa may be the major area which needs further detailed investigation. It should be pointed out that NMSim does not provide a quantitative description of the distribution of the generated conformations, nor does it provide conformational energies. Such energies may be obtained by other molecular mechanics calculations using the NMSim-generated conformations as inputs.

Using two-dimensional itemization of the rigidity index, a stability map is derived by identifying 'rigid contacts' between two residues presented by their Cα atoms[32]. It shows that a rigid contact exists if two residues belong to the same rigid cluster. The microscopic stabilities of all residue-residue contacts come into a stability map. Thus, for toxin Cry1Aa, the stability map represents the distribution of flexibility and rigidity within the toxin. This pairwise stability information is consistent with the foregoing local flexibility index shown in Figure 2.

CONCLUSION

CNA and NMSim are user-friendly interfaces for flexibility analysis that offer very detailed information on thermalstability, flexibility, and function. This study showed that the decrease in Cry1Aa network rigidity with increasing temperature was evident. Two phase transition points in which the Cry1Aa structure lost rigidity during simulation were identified. Two rigid clusters were found in the domain I and II, and weak spots were in the C-terminal domain III. Although several flexible regions were found in all the three domains, the most flexible regions were in the apical loops of domain II. Our results may be helpful in understanding the action mode of Bt toxins and molecular design for increasing its thermostability.

ACKNOWLEDGEMENT

We thank ZHANG You Min (Gene Bridge GmbH, Dresden, Germany) for the critical reading of this manuscript.

Received: April 10, 2015;
Accepted: August 1, 2015

REFERENCES

1. Schellman JA. Macromolecular binding. Biopolymers, 1975; 14, 999-1018.
2. Daniel RM, Dunn RV, Finney JL, et al. The role of dynamics in enzyme activity. Annu Rev Biophys Biomol Struct, 2003; 32, 69-92.
3. Kaarsholm NC, Ko HC, Dunn MF. Comparison of solution structural flexibility and zinc binding domains for insulin, proinsulin, and miniproinsulin. Biochem, 1989; 28, 4427-35.
4. Keller D, Clausen R, Josefsen K, et al. Flexibility and bioactivity of insulin: an NMR investigation of the solution structure and folding of an unusually flexible human insulin mutant with increased biological activity. Biochem, 2001; 40, 10732-40.
5. Vihinen M. Relationship of protein flexibility to thermostability. Protein Eng, 1987; 1, 477-80.
6. Cozzini P, Kellogg GE, Spyrakis F, et al. Target flexibility: an emerging consideration in drug discovery and design. J Med Chem, 2008; 51, 6237-55.
7. McCammon JA, Gelin BR, Karplus M. Dynamics of folded proteins. Nature, 1977; 267, 585-90.
8. Gohlke H, Kuhn L, Case DA. Change in flexibility upon complex formation: Analysis of Ras-Raf using molecular dynamics and a molecular framework approach. Proteins, 2004; 56, 322-37.
9. Lindahl E, Azuara C, Koehl P, et al. NOMAD-Ref: visualization, deformation and refinement of macromolecular structures based on all-atom normal mode analysis. Nucleic Acids Res, 2006; 34, W52-6.
10. Suhre K, Sanejouand YH. ElNemo: a normal mode web server for protein movement analysis and the generation of templates for molecular replacement. Nucleic Acids Res, 2004; 32, W610-4.
11. Camps J, Carrillo O, Emperador A, et al. FlexServ: an integrated tool for the analysis of protein flexibility. Bioinformatics, 2009; 25, 1709-10.
12. Hollup SM, Sælensminde G, Reuter N. WEBnm@: a web application for normal mode analysis of proteins. BMC Bioinformatics, 2005; 6, 52.
13. Eyal E, Yang LW, Bahar I. Anisotropic network model: systematic evaluation and a new web interface. Bioinformatics, 2006; 22, 2619-27.
14. Lopez-Blanco JR, Aliaga JI, Quintana-Orti ES, et al. iMODS: internal coordinates normal mode analysis server. Nucleic Acids Research, 2014; 42, W271-6.
15. Frappier V, Chartier M, Najmanovich RJ. ENCoM server: exploring protein conformational space and the effect of mutations on protein function and stability. Nucleic Acids Res, 2015; 43, W395-400.
16. Pfleger C, Rathi PC, Klein DL, et al. Constraint Network Analysis (CNA): A Python software package for efficiently linking biomacromolecular structure, flexibility, (thermo-) stability, and function. J Chem Inf Model, 2013; 53, 1007-15.
17. Krüger DM, Ahmed A, Gohlke H. NMSim Web Server: integrated approach for normal mode-based geometric simulations of

biologically relevant conformational transitions in proteins. Nucleic Acids Res, 2012; 40, W310-W316.

18.Bravo A, Gómez I, Porta H, et al. Evolution of *Bacillus thuringiensis* Cry toxins insecticidal activity. Microb Biotechnol, 2013; 6, 17-26.

19.Jenkins JL, Dean DH. Binding specificity of *Bacillus thuringiensis* Cry1Aa for purified, native *Bombyx mori* aminopeptidase N and cadherin-like receptors. BMC Biochem, 2001; 2, 1-7.

20.Xu C, Wang BC, Yu Z, et al. Structural insights into *Bacillus thuringiensis* Cry, Cyt and parasporin toxins.Toxins (Basel), 2014; 6, 2732-70.

21.Bravo A, Gill SS, Soberon M. Mode of action of *Bacillus thuringiensis* Cry and Cyt toxins and their potential for insect control. Toxicon, 2007; 49, 423-35.

22.Walters FS, Slatin SL, Kulesza CA, et al. Ion channel activity of N-terminal fragments from CryIA(c) delta-endotoxin. Biochem Biophys Res Commun, 1993; 196, 921-6.

23.Lee MK, Rajamohan F, Jenkins JL, et al. Role of two arginine residues in domain II, loop 2 of Cry1Ab and Cry1Ac *Bacillus thuringiensis* delta-endotoxin in toxicity and binding to *Manduca sexta* and *Lymantria dispar* aminopeptidase N. Mol Microbiol, 2000; 38, 289-98.

24.Nishimoto T, Yoshisue H, Ihara K, et al. Functional analysis of block 5, one of the highly conserved amino acid sequences in the 130-kDa CryIVA protein produced by *Bacillus thuringiensis* subsp. israelensis. FEBS Lett, 1994; 348, 249-54.

25.Lee MK, You TH, Gould FL, et al. Identification of residues in domain III of *Bacillus thuringiensis* Cry1Ac toxin that affect binding and toxicity. Appl Environ Microbiol, 1999; 65, 4513-20.

26.Rader AJ, Hespenheide BM, Kuhn LA, et al. Protein unfolding: rigidity lost. Proc Natl Acad Sci USA, 2002; 99, 3540-5.

27.Krüger DM, Rathi PC, Pfleger C, et al. CNA web server: rigidity theory-based thermal unfolding simulations of proteins for linking structure, (thermo-) stability, and function. Nucleic Acids Res, 2013; 41, 340-8.

28.Radestock S, Gohlke, H. Protein rigidity and thermophilic adaptation. Proteins, 2011; 79, 1089-108.

29.Radestoc S, Gohlke H. Exploiting the link between protein rigidity and thermostability for data-driven proteinengineering. Eng Life Sci, 2008; 8, 507-22.

30.Ahmed A, Rippmann F, Barnickel G, et al. A normal mode-based geometric simulation approach for exploring biologically relevant conformational transitions in proteins. J Chem Inf Model, 2011; 51, 1604-22.

31.Jacobs DJ, Rader AJ, Kuhn LA, et al. Protein flexibility predictions using graph theory. Proteins, 2001; 44, 150-65.

32.Pfleger C, Radestock S, Schmidt E, et al. Global and local indices for characterizing biomolecular flexibility and rigidity. J Comp Chem, 2013; 34, 220-33.

33.Andraud C, Beghdadi A, Lafait J. Local Entropy Characterization of Correlated Random Microstructures. Physica A, 1994; 207, 208-12.

34.Schwartz JL, Juteau M, Grochulski P, et al. Restriction of intramolecular movements within the Cry1Aa toxin molecule of *Bacillus thuringiensis* through disulfide bond engineering. FEBS Lett, 1997; 410, 397-402.

35.Rajamohan F, Cotrill JA, Gould F, et al. Role of domain II, loop 2 residues of *Bacillus thuringiensis* CryIAb delta-endotoxin in reversible and irreversible binding to *Manduca sexta* and *Heliothis virescens*. J Biol Chem, 1996; 271, 2390-6.

36.Zhao XM, Xia LQ, Ding XZ, et al. The theoretical three-dimensional structure of *Bacillus thuringiensis* Cry5Aa and its biological implications. Protein J, 2009; 28, 104-11.

37.Fujii Y, Tanaka S, Otsuki M, et al. Cry1Aa binding to the cadherin receptor does not require conserved amino acid sequences in the domain II loops. Biosci Rep, 2013; 33, e00010.

38.Vandemeulebroucke A, De Vos S, Van Holsbeke E, et al. A flexible loop as a functional element in the catalytic mechanism of nucleoside hydrolase from *Trypanosoma vivax*. J Biol Chem, 2008; 283, 22272-82.

39.Zgiby S, Plater AR, Bates MA, et al. A functional role for a flexible loop containing Glu182 in the class II fructose-1,6-bisphosphate aldolase from *Escherichia coli*. J Mol Biol, 2002; 315, 131-40.

40.Wang FX, Xia LQ, Ding XZ, et al. N546 in 18-19 loop is important for binding and toxicity of the *Bacillus thuringiensis* Cry1Ac toxin. J Invertebr Pathol, 2009; 101, 119-23.

41.Xia LQ, Wang FX, Ding XZ , et al. The role of 18-19 loop structure in insecticidal activity of Cry1Ac toxin from *Bacillus thuringiensis*. Chin Sci Bull, 2008; 53, 3178-84.